European Journal of Radiology 85 (2016) 1765–1772

Contents lists available at ScienceDirect

European Journal of Radiology

journal homepage: www.elsevier.com/locate/ejrad

Differentiation of benign and malignant lung lesions: Dual-Energy Computed Tomography findings

Víctor González-Pérez[a], Estanislao Arana[b,*], María Barrios[b], Albert Bartrés[a], Julia Cruz[c], Rafael Montero[d], Manuel González[b], Carlos Deltoro[b], Encarnación Martínez-Pérez[e], Karol De Aguiar-Quevedo[f], Miguel Arrarás[f]

[a] Dept Radiophysics, Foundation IVO, Valencia, Spain
[b] Dept Radiology, Foundation IVO, Valencia, Spain
[c] Dept Pathology, Foundation IVO, Valencia, Spain
[d] GE Healthcare Diagnostic Imaging, Iberia, Spain
[e] Dept Pneumology, Foundation IVO, Valencia, Spain
[f] Dept Thoracic Surgery, Foundation IVO, Valencia, Spain

ARTICLE INFO

Article history:
Received 23 May 2016
Received in revised form 22 July 2016
Accepted 26 July 2016

Keywords:
Lung neoplasms
Granuloma
Carcinoma
Non-small-cell lung
Small cell lung carcinoma
Dual-Energy Multidetector Computed Tomography
Image processing
Computer-assisted

ABSTRACT

Purpose: To determine whether parameters generated by Dual-Energy Computed Tomography (DECT) can distinguish malignant from benign lung lesions.
Methods: A prospective review of 125 patients with 126 lung lesions (23 benign and 103 malignant) who underwent lung DECT during arterial phase. All lesions were confirmed by tissue sampling. A radiologist semi-automatically contoured lesions and placed regions of interest (ROIs) in paravertebral muscle (PVM) for normalization. Variables related to absorption in Hounsfield units (HU), effective atomic number (Z_{eff}), iodine concentration (ρ_I) and spectral CT curves were assessed. Receiver operating characteristic (ROC) curves were generated to calculate sensitivity and specificity as predictors of malignancy. Multivariate logistic regression analysis was performed.
Results: Reproducibility of measures normalized with PVM was poor. Bivariate analysis showed minimum Z_{eff} and normalized mean Z_{eff} to be statistically significant ($p = 0.001$), with area under the curve (AUC) values: 0.66 (CI 95% 0.54–0.80) and 0.72 (CI 95%, 0.60–0.84), respectively. Logistic regression models showed no differences between raw and normalized measurements. In both models, minimum HU (OR: 0.9) and size (OR: 0.1) were predictive of benign lesions.
Conclusions: A quantitative approach to DECT using raw measurements is simpler than logistic regression models. Normalization to PVM was not clinically reliable due to its poor reproducibility. Further studies are needed to confirm our findings.

1. Introduction

Lung cancer remains the leading cause of cancer-related death in both males and females [1]. In patients with suspected lung cancer, the mainstay examination is a contrast-enhanced CT of the thorax and upper abdomen. Dual-Energy Computed Tomography (DECT) has recently appeared as a tool for quantifying iodine concentration. Studies have shown its utility in differentiating benign from malignant lesions in lung [2–4] as well as other locations [5–9].

On a DECT scanner, simultaneous data sets for two energy spectra (usually 80 and 140 kVp) are obtained in the same acquisition. Gemstone spectral imaging (GSI) acquires images with fast switching between both energy levels [10].

GSI creates a spectral curve that displays the attenuation of tissue in HU units across the 40- to 140-keV monochromatic energy range, and displays reconstructed images for quantitative iodine content (ρ_I) and effective atomic number (Z_{eff}). Z_{eff} represents the composite atom for a mixture of various materials and characterizes tissue composition. To date, only one previous in vivo study has employed Z_{eff} to differentiate benign from malignant thyroid nodules [8].

Regarding lung lesions and DECT, several parameters have been studied: ρ_I to distinguish inflammatory from malignant masses [2],

* Corresponding author at: Dept Radiology, Fundación IVO, Prof Beltrán Báguena, 11, 46009 Valencia, Spain.
E-mail address: aranae@uv.es (E. Arana).

http://dx.doi.org/10.1016/j.ejrad.2016.07.019
0720-048X/

virtual non-enhanced iodine images to characterize solitary pulmonary nodules and granuloma [3,12]; and slope of spectral HU curves to differentiate benign from malignant tumors [2,4].

Quantitative studies with DECT have also been employed in other locations: differentiating benign from malignant neck pathologies [5], osteoblastic metastases from bone island [6], squamous cell carcinoma [7], thyroid nodules [8] and renal masses [9].

Most of these studies are based on two-dimensional ROIs, usually placed at discretional intralesional sites [2,11]. Software technology allows highly accurate lung lesion segmentation [12]. Recently, 3D segmentation has been applied, associating iodine content with tumor differentiation [13].

Our aim was to prospectively evaluate if spectral HU curves, ρ_I, Z_{eff} and HU parameters are able to differentiate between benign and malignant lesions in lung.

2. Material and methods

2.1. Baseline population

From July 2013 to February 2015, a total of 125 patients (84 men, 41 women); age range, 20–88 years; mean age, 64.9 years ± 12.24 [standard deviation], were prospectively enrolled. Patients were referred from a lung cancer screening unit, cancer hospital departments and primary care clinics. All patients signed informed consent on admission for treatment and research. The study was approved by the ethics committee of our hospital.

2.2. CT examinations

CT examination was performed on a Discovery CT 750 HD scanner (GE Healthcare, WI, USA). Patients were injected with 1.35 ml/kg of body weight of nonionic iodinated contrast material (Iopamidol, 300 mg/ml; Bracco, Italy) via the antecubital vein at a rate of 4.0 ml/s. A GSI exam of the entire chest was performed with a scan delay of 35 s after the start of contrast injection during arterial phase (AP) followed by a non GSI thoracic-abdominal exam in portal venous phase (PVP), 30 s after AP for tumor staging. Acquisition parameters for the first phase (thorax) were: helical tube rotation time 0.5 s, tube current 630 mA, helical pitch 1.375, SFOV 500 mm and collimation 40 mm. 2.5 and 1.25 mm thickness contiguous axial images were generated with a soft tissue kernel (standard) monochromatic with GSI data file at a default energy level of 70 KeV. For the thorax-abdomen study parameters were: helical tube rotation time 0.5 s, 3D mA modulation (SmartmA) with a noise index of 20 for 5 mm initial images, helical pitch 1.375, SFOV 500 mm and collimation 40 mm. 2.5 thickness contiguous axial images were generated with a soft tissue Kernel (standard) with an iteration level (ASiRTM®) of 40%. CT Dose Index vol (CTDIvol) for GSI acquisition was of 12.72 mGy.

2.3. Quantitative analysis of dual-energy findings

Lesion volume was semi-automatically segmented using Dexus® lung nodule function (ADW4.6; GE Healthcare, USA) by two radiologists (EA and MB with 18 and 11 years of experience in chest CT respectively) blinded to patient data. The same radiologists independently measured the quantitative parameters. Intra- and inter-observer reliability was evaluated in 20 randomly selected patients.

To minimize the effect of body weight, circulation status and body composition, lung mass measurements were normalized to paravertebral musculature (PVM) values. PVM was contoured with a 2.5 mm diameter two-dimensional ROI on the same image as the heart septum.

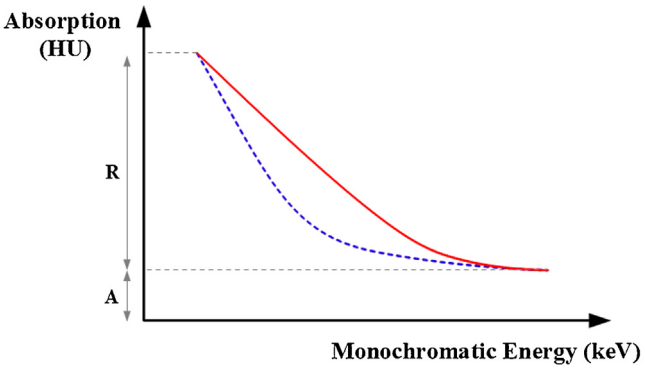

Fig. 1. Example of two spectral curves. A is the asymptote of the curve (the value the curve is approaching as the keV increases); R is the HU variation range within the 40–140 keV monochromatic energy interval and C is a variable which describes curve slope. In this example, dashed curve has a higher C value than continuous curve.

Mean, maximum and minimum values for HU, ρ_I and Z_{eff} were registered for lesions and control ROIs.

Following previously described methodology [5], spectral curves were parameterized as a decreasing exponential with three parameters (A: asymptote, R: range, C: decay).

$$Y = A + Re^{\frac{-C(keV-40)}{100}}$$

where Y is the attenuation in HU. A graphical explanation of curve parameterization used is shown in Fig. 1.

Spectral HU curves were created for lung lesion and left PVM with GSI Viewer. MATLAB R2010a software (The Mathworks, Natick, MA, USA) was used for curve parametrization. A non-linear least squares method was used to fit each curve to the model.

Differences between benign and malignant cohorts were evaluated. A specific analysis for the small lesion (<3.9 cm^3) sub-cohort was also performed since tumors below this threshold show significant correlation between blood-perfusion and standardized uptake value in FDG-PET studies [14]. Larger tumors usually show a heterogeneous metabolic pattern, not fully ascertained by either CE-CT or FDG-PET [14].

Regarding spectral curves, we assessed the lesional parameters A, R and C, as well as the A, R and C values minus their respective PVM values. HU, ρ_I (iodine content) and Z_{eff} were also evaluated, both raw and normalized to mean PVM values. Mean, maximum and minimum values at each 3D ROIs were taken as described in Fig. 2. In total 24 variables were analyzed, as shown in Tables 2 and 3.

2.4. Statistical analysis

To minimize the influence of extreme values or non-normal distributions, data were transformed using a Box-Cox power transformation by Statistica 12 (Dell Inc, Round Rock, TX, USA). In Box-Cox transformation the transformed variables are:

$$Y_i^{(\lambda)} = K_1\left(Y_i^{\lambda} - 1\right) \text{if} \lambda \neq 0$$

$$Y_i^{(\lambda)} = K_2 \ln\left(Y_i\right) \text{if} \lambda = 0$$

Bilateral statistical analysis was performed using the Mann-Whitney *U* test [15], with a Bonferroni adjustment for multiple comparisons. Significance was set at $p < 0.002$. Receiver operating characteristic (ROC) curves were generated and diagnostic capability was determined by calculating the area under the ROC curve (AUC), as shown in Tables 2 and 3.

For reliability analysis, diameter, volume and GSI measurements of lung lesions and PVM ROIs were analyzed using the Intraclass